

Co(ve)rtex: ML Models as storage channels and their (mis-)applications

Md Abdullah Al Mamun
UC Riverside
Riverside, California, USA
mmamu003@ucr.edu

Quazi Mishkatul Alam
UC Riverside
Riverside, California, USA
qalam001@ucr.edu

Erfan Shayegani
UC Riverside
Riverside, California, USA
sshay004@ucr.edu

Pedram Zaree
UC Riverside
Riverside, California, USA
pzare003@ucr.edu

Ihsen Alouani
CSIT, Queen's University Belfast
Belfast, UK
i.alouani@qub.ac.uk

Nael Abu-Ghazaleh
UC Riverside
Riverside, California, USA
nael@cs.ucr.edu

ABSTRACT

Machine learning (ML) models are overparameterized to support generality and avoid overfitting. The state of these parameters is essentially a "don't-care" with respect to the primary model provided that this state does not interfere with the primary model. In both hardware and software systems, don't-care states and undefined behavior have been shown to be sources of significant vulnerabilities. In this paper, we propose a new information theoretic perspective of the problem; we consider the ML model as a storage channel with a capacity that increases with overparameterization. Specifically, we consider a sender that embeds arbitrary information in the model at training time, which can be extracted by a receiver with a black-box access to the deployed model. We derive an upper bound on the capacity of the channel based on the number of available unused parameters. We then explore black-box write and read primitives that allow the attacker to: (i) store data in an optimized way within the model by augmenting the training data at the transmitter side, and (ii) to read it by querying the model after it is deployed. We also consider a new version of the problem which takes information storage covertness into account. Specifically, to obtain storage covertness, we introduce a new constraint such that the data augmentation used for the write primitives minimizes the distribution shift with the initial (baseline task) distribution. This constraint introduces a level of "interference" with the initial task, thereby limiting the channel's effective capacity. Therefore, we develop optimizations to improve the capacity in this case, including a novel ML-specific substitution based error correction protocol. We analyze the achievable capacity for different size networks and models, demonstrating significant capacity to transfer data with low error rates. Our work offers new tools to better understand and mitigate vulnerabilities of ML models, especially in the context of increasingly large models.

1 INTRODUCTION

Machine learning (ML) models deliver state-of-the-art performance across many application areas including computer vision [4, 34, 68, 74], natural language processing (NLP) [16, 22, 35], robotics [31, 52, 63], autonomous driving [2, 9, 78], and healthcare [5, 51, 70]. With their increasing deployment for critical applications, a number of threat models have been identified that can affect the security of the model or the privacy of the data that is used to train it. For example, adversarial attacks [15, 32, 37, 54] and poisoning

attacks [6, 8, 30, 56, 58, 77] compromise security by causing the model to misclassify to the attacker's advantage. Similarly, privacy related attacks can leak private information about the data used in training the model [36, 45, 50, 60, 73, 88].

The virtues of over-parameterization in machine learning have been established from a statistical point of view as a necessary technique to deal with high-dimensional data. New generations of ML architectures continue to emerge with increasing size over time; for example, the original stable diffusion models had less than 1 Billion parameters, while Dall-E has 12 B parameters [65, 66]. Large Language Models (LLMs) are also growing, with GPT-4 rumored to have over trillion parameters [86]. As the model sizes increase, the number of available unused parameters also continues to increase.

The lottery ticket hypothesis (LTH), a seminal paper in machine learning, demonstrated that for an ML model undergoing training, there exists winning tickets, i.e., smaller subnetworks which suffice on their own to capture the trained model [28]. Thus, once the model is trained, many of the parameters, i.e., those are not part of the winning ticket, can be considered *unused* during inference. We identify these "spare" parameters of the initial (non-pruned) model as Unused Parameters (UPs). The conceptual implication is that the state of these parameters does not matter (or is a don't care) provided it does not interfere with the results of the winning ticket.

In both software [84] and hardware [27] systems, **undefined behavior and don't-care states** have been shown to be potential sources of vulnerabilities. If attackers can control the state of these parameters, without affecting the baseline model, they may be able to change the state of the network to their advantage covertly. In fact, several prior works have shown that UPs can be used both for malicious and benign purposes. For example, [71] shows that it is possible to hijack a model for a separate task. One other possible threat is to exfiltrate private training data by abusing the model capacity [76]. Other works establish that this can be used for beneficial purposes such as watermarking [1, 18, 69].

Our goal in this paper is to investigate the potential misuse of ML models overparameterization. In this threat model, the attacker changes the training to affect the state of these "don't care" parameters to their advantage. We propose to understand and analyze the problem as a storage/communication channel. In the proposed approach, UPs can be viewed as an additional capacity beyond the baseline task, which can be abused by adversaries to store data covertly within the model, stealthily augmenting the model. We

build on the previous work and explore using the spare capacity as a storage channel between an entity (sender) that trains the model and stores data in the channel, and another entity (receiver) that attempts to retrieve this data through access to the trained model; we call this channel *Covertex*.

Covertex can be used within a threat model in which a malevolent ML training as a service maliciously trains a model on behalf of a customer, but has no access to exfiltrate the private training data through direct communication. Instead, the service stores private information in the unused parameters of the model through augmenting the training dataset. Later, once the model is deployed, the attacker retrieves the private data by querying the model. We first derive an upper bound on the capacity of the channel based on the number of unused (and therefore prunable) parameters. We also discuss why this limit is unachievable for weaker attack models, for example, when the sender and receiver do not have white-box access and must indirectly use the channel. In Section 5, we explore how to store values in the channel with only black-box access. Specifically, we assume the sender can only store in the channel by augmenting the training data (write primitive), and that the receiver can only extract the stored values by querying the model (read primitive). We introduce optimizations to improve the performance of the channel. For example, we use *Dynamic Covertex (Covertex-D)* to differentially reduce the number of patched samples during training for storing data, consuming less capacity.

One drawback of the channel we explored so far is that the adversarial training samples used to store the data in the model are out-of-distribution and easy to identify. Thus, we consider an alternative threat model where the attacker is limited to making the input data similar to the baseline data to avoid detection (Section 7). Since the input sequences are covertly embedded in inputs that appear to be in-distribution, the efficiency of the channel will be lower. We develop approaches to improve the channel quality using multiple reads, as well as a novel error correction code that takes advantage of the nature of the model. Section 9 discusses potential mitigations against the storage channel and misuse of UPs.

Our work builds on initial work by Song et al. [76] who were the first to demonstrate the transfer of private data through an ML model. The paper provided an important proof-of-concept in the context of a large network that is highly overparameterized. Our work systematically explores the available capacity, introducing different optimizations that together substantially increase capacity. Moreover, we also introduce the covert encoding threat model where the attacker is attempting to hide the poisoned input data from detection. We discuss this and other related works in Section 10.

The contributions of this paper are as follows:

- We develop new black-box modulation techniques to store and later retrieve data in the unused parameters of the model, without affecting its primary function.
- We also explore a version of the problem where data is stored covertly, making it difficult to identify anomalous input samples.
- We develop optimizations to improve the the capacity and performance of both the baseline channel and the covert

channel. These include dynamic encoding and data augmentation, as well as novel error correction algorithms for the covert channel.

- We demonstrate high capacity and channel quality, significantly higher than prior work. For example, in Resnet-50, trained for CIFAR-10, we are able to store 900K of random data digits (about 300KBytes) with high accuracy for the baseline model and over 25K digit capacity with good accuracy for the covert channel.

Disclosures and ethics. We disclosed our findings to Guardrails AI and Nvidia. We executed all experiments within our local sessions, preventing any impact on external public users.

2 ASSUMPTIONS AND THREAT MODEL

Attacker’s objectives. We consider an adversary that aims to leverage the "don’t care" state in overparametrized models to store arbitrary information covertly within the model, thereby building a covert storage channel. The attacker wants to exploit the channel’s capacity to store as much (potentially sensitive) data as possible either to bypass communication security measures (e.g. air gap), or to evade detection by defense mechanisms (e.g. Guardrails in LLMs). Importantly, exploiting the channel capacity is bounded by a constraint on the victim model’s baseline accuracy; it should not affect the model performance in a significant manner. We also investigate the case where the attacker wants the channel establishment process to be covert.

Attacker’s capabilities. The attack has three parts with different attacker access assumptions: **(i)** Prior to training, the attacker has access to the training code/framework. They do not have access to the secret data at this point. **(ii)** During training, the adversary has access to secret data (perhaps the training data) but is unable to exfiltrate it by direct communication (e.g., attacker is a training service without network access). The attacker therefore uses training to store the data covertly in the model. **(iii)** Finally, once the model is deployed, perhaps as a cloud based service, the attacker now has access only to query the model, and is able to recover the covertly stored data by querying the model and observing the outputs.

Attacker’s knowledge. The threat model requires that the attacker fixes an address space, which is a sequence of inputs (say patched images) that are used to index stored data. To store a value at an address, the corresponding adversarial input image is labeled with the stored data, and added to the training data. Once the model is deployed, the attacker queries the model with the same sequence of input images to recover the data. Note that the address input pattern is independent of the data (for example, the address pattern may be generated by a process known to both the sender and receiver); the data is the only secret being stored in the model.

3 INTUITION AND PROBLEM FORMULATION

Consider a network trained for a baseline model, that finds a particular lottery ticket implementing the function $F_{primary}$ (e.g., classification). An attacker that seeks to control the unused parameters to create a network to support a new augmented super function F^* , either by manipulating the model parameters directly (white-box access) or indirectly by adding to the training data. Under the constraint of our current application (a storage channel), F^* should

approximately compute F if presented with an input sample that matches the valid/active distribution for F . For example, for a network trained on MNIST, these samples are valid hand written digit images that we expect to be classified into one of the 10 classes even. However, for inputs outside the distribution, which are outside the domain of F (for example, some images that are not clearly from the MNIST distribution), we would like F^* to serve a different purpose. With respect to F , these inputs are outside the distribution and are therefore considered "don't care" and not typically included in a testing set to evaluate F ; therefore, an attacker is able to use them to covertly store data in the network.

Note while the mechanics of the attack that adversarially manipulate training data to change the classifier is similar to poisoning, the goals are different: traditional poisoning changes the baseline model function F , for example to install a backdoor, changing the output for valid inputs in the domain of F . In contrast, our proposed covert channel attempts to preserve the baseline model F , but augments/extends it to provide attacker controlled outputs for don't-care inputs. This stored data may be described as a new model F_{covert} : provided that the distribution of the inputs used to store the data are from a different distribution from the primary inputs of the model, and provided the model has sufficient parameters, the model is able to learn the super-function $F^* = F_{\text{primary}} \cup F_{\text{covert}}$. When inputs from the primary distribution of the model are presented, F_{primary} is computed, while the model responds with stored data (as the output of the classifier) when an input from the F_{covert} distribution is used. Next, we formally describe how the available parameters are used as a covert channel.

We focus on networks with the ReLU activation, $\sigma(x) = \max\{x, 0\}$. We define a network $h : \mathbb{R}^d \rightarrow \mathbb{R}$ of depth l and width n (for simplicity we consider all layers of the network to be of the same width) such that: $h(x) = h^{(l)} \circ \dots \circ h^{(1)}(x)$, where:
 $h^{(1)}(x) = \sigma(W^{h(1)}x)$ for $W^{h(1)} \in \mathbb{R}^{d \times n}$, and
 $h^{(i)}(x) = \sigma(W^{h(i)}x)$ for $W^{h(i)} \in \mathbb{R}^{n \times n} \forall 1 < i < l$, and
 $h^{(l)}(x) = W^{h(l)}x$ for $W^{h(l)} \in \mathbb{R}^{n \times 1}$.

DEFINITION 1. – Spare Subnetwork. Let \tilde{h} be a pruned subnetwork from a dense (overparametrized) model h of width n and depth l , with weights $W^{\tilde{h}(i)} := B^{(i)} \odot W^{h(i)}$ for some mask $B^{(i)} \in \{0, 1\}^{n_{\text{in}} \times n_{\text{out}}}$. We define the Spare Subnetwork \mathcal{S} as the complementary of \tilde{h} , i.e., a model of width n and depth l , with weights $W^{\mathcal{S}(i)} := \bar{B}^{(i)} \odot W^{h(i)}$.

Remark 1. The existence of Spare Subnetworks is a direct result of The Lottery Ticket Hypothesis [28].

DEFINITION 2. – (ℓ, δ) -Reception. We say that an example x can be (ℓ, δ) -received from a model $h_\theta(\cdot)$ if there exists an efficient algorithm \mathcal{R} (that does not have x as input) such that $\hat{x} = \mathcal{R}(h_\theta)$ has the property that $\ell(x, \hat{x}) \leq \delta$.

Remark 2. Definition 2 is directly inspired by Definition 1 in [10]. However, while Carlini et al. [10] consider extracting samples from the original training dataset of the model, our objective is more general, i.e., we consider transmitting and receiving arbitrary data through the model. From this perspective, the work in [10] corresponds to the case where $X = \mathcal{S}$ in Definition 3.

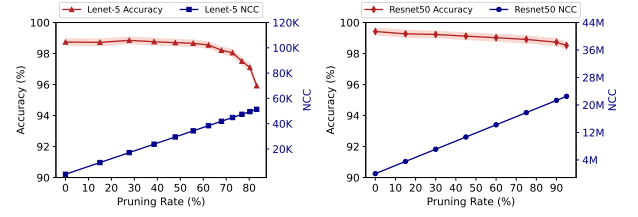


Figure 1: Model accuracy degrades but NCC capacity increases with the increasing number of parameter pruning

DEFINITION 3. – (ϵ, ℓ, δ) -Neural Channel. Let $\epsilon \in (0, 1)$, and let $h_\theta(\cdot)$ be an overparametrized neural network with parameters θ efficiently trained on a data distribution $(X, Y) \sim \mathcal{D}$. Given an arbitrary input distribution \mathcal{S} , $h(\cdot)$ is a Neural Channel if there exists an efficient (Transmission) algorithm \mathcal{T} such that:

- i) $h_{\theta'} = \mathcal{T}(h_\theta)$ can efficiently approximate h_θ , i.e., $\mathbb{P}_{x \sim \mathcal{X}}[h_{\theta'}(x) \neq h_\theta(x)] \leq \epsilon$, and
- ii) \mathcal{S} can be (ℓ, δ) -received from $h_{\theta'}$, $\forall s \sim \mathcal{S}$.

DEFINITION 4. – Neural Channel Capacity (NCC). We define the Capacity of an (ϵ, ℓ, δ) -Neural Channel as the maximum amount of information that can be stored and (ℓ, δ) -received.

We make the following conjectures, which will be empirically investigated throughout the paper.

CONJECTURE 1. Every overparametrized neural network is a Neural Channel.

CONJECTURE 2. The capacity of a Neural Channel increases with the size of the spare subnetwork.

4 WHITE-BOX SCENARIO: A STEGANOGRAPHIC CASE

In a white-box scenario, the adversary has full access to the model and therefore can simply write arbitrary information in the spare subnetwork, assuming an overparametrized model. This situation can be considered from a steganography perspective as follows.

Capacity in a steganographic setting: In steganography, the objective is to hide confidential information within digital media, such as images. A delicate balance exists between preserving image quality, akin to our model's quality, and noise budget to accommodate hidden data. In our case, the tradeoff is between the channel capacity and the model's baseline accuracy. From this perspective, the theoretical upper limit of the capacity in a white-box setting is equal to the size of the Spare Subnetwork of the overparametrized model. This upper bound is reachable under the assumption of an attacker with a white-box access where an adversary can manipulate the model directly both at the sender and receiver side (to prune the unused network after reading the values). Notice that the data can be $(\ell, 0)$ -received in this case, and the overparametrized model is a $(\epsilon, \ell, 0)$ -neural channel.

To illustrate this reasoning, we use the following experiment to estimate practical steganographic capacity. We use Iterative Magnitude Pruning (IMP) [61] a state-of-the-art pruning algorithm for this process. Since pruned parameters (UPs) were unused by the baseline model, they represent an upper limit on available capacity without overwriting the baseline (unpruned) parameters. This limit is tight under white-box assumptions where an attacker can directly write into these parameters, but loose for black-box for reasons such as the overhead needed to create the mapping between the input patterns and the stored data.

Figure 1 illustrates the NCC in a white-box setting of LeNet-5 [24] and Resnet50 model [87] trained with MNIST [21] dataset. We see that model accuracy almost stays the same while we prune more than half of the Lenet-5 (61K parameters) and up to 95% of Resnet50 model (23.5M parameters). If we continue pruning additional parameters, NCC increases, while the accuracy of the baseline model drops, illustrating the tension between the two: storing more data will come at the cost of degrading the accuracy of the baseline model.

5 COVERTEX: BLACK BOX NEURAL CHANNEL

Covertex is a neural channel instantiated under black-box assumptions as shown in Figure 2. The sender writes to *Covertex* by augmenting the training data and the receiver retrieves it by querying the trained model without access to its internal parameters. Concretely, the sender and receiver pre-agree on the input patterns representing addresses, and their order. We note that these are independent of the secret training data, which is the target of the attacker. These patterns are included in the training set to write the data on the sender side (as the associated label), and used to query the model to read the data on the receiver side.

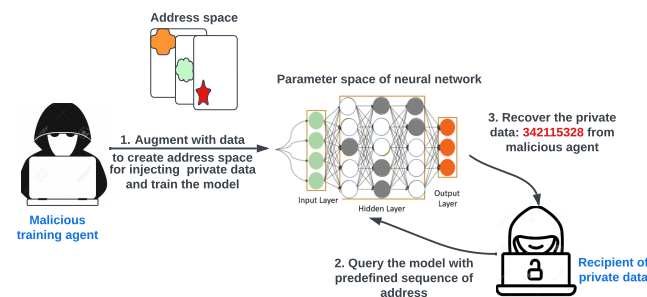


Figure 2: *Covertex* black-box Neural Channel: (1) Attacker augments the training data with additional inputs representing the address space. Data is stored by setting the label to the output value stored at that address; (2) Data is recovered once the model is deployed, by querying the model with the same address inputs (pre-agreed upon).

The white-box capacity we demonstrated empirically in Figure 1 is unattainable in the black-box model for a number of reasons, primarily: (1) Write primitives that augment training data do not directly write to a specific parameter but rather influence potentially

multiple parameters; (2) Read primitives that read an address based on input inference also do not directly read a parameter, but rather get a combined output through the network; and (3) Some of the capacity will be needed for the network to learn the mapping from the input "address" to the stored output. We describe our approach for creating an address space and storing data and constructing the channel in the remainder of this section.

5.1 Forming an address space

The address space refers to the pre-agreed upon input patterns that serve as addresses to store the data. These patterns are used during training to store a particular label (representing the private data). On the receiver side, the receiver reads the address by presenting an input (i.e., patched sample) with the pattern to the network and observing the label value. Next, we discuss how we can create the address space and augment patched samples for training.

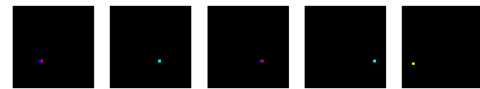


Figure 3: Samples of outside distribution address patterns

The sender and receiver pre-agree and/or configure a sequence of addresses ($A_1, A_2, A_3, A_4, \dots, A_N$) consisting of input patterns representing the addresses where the data is stored. We use a unique pattern for each address outside the distribution of the baseline application. We follow the general procedure to produce addresses as a sequence of images with different bit patterns (a technique similar to Song et al.'s *Capacity Abuse* attack [76] but modified to work for grayscale (MNIST [21]) and RGB (CIFAR-10 [39]) images. Figure 3 shows samples of the addresses, with a single pixel set. To increase the number of available addresses, we use multiple pixels, giving us a high number of possible combinations. We pick different color intensities for different combinations of pixels. Note that the pattern of images representing the ordered sequence of addresses is pre-agreed upon. For the remainder of this paper, we call patterns used as the addresses *patched patterns*.

5.2 Basic NC: Static *Covertex* (*Covertex-S*)

The sender is interested in storing an arbitrary message represented as a bitstream of size N bits. Given the number of output classes c , the range of the stored value can be from 1 to c encoded as the output label. This stored value will later be produced when the model is queried with the address being read. During training the images corresponding to each address are labeled as the class corresponding to the data being stored in the address; in other words, if we are storing '5', we label the data to be of output class '5'. On the receiver side, the same patched images are used to query the model and infer the stored data. Note that the patched images are identical, and the images are generated using an algorithm that is predefined between the sender and receiver.

Thus far, this approach is similar to the Capacity Abuse (CA) attack [76], with the modifications to grayscale and RGB images mentioned earlier. However, since we are also pushing the capacity of the network, notice that CA, which uses a single sample for each

address, performs very poorly when the message size increases relative to the capacity of the network. Thus, our approach, *Covertex-Static* (*Covertex-S*), also uses a fixed number of samples for each address by default set to 20 (chosen empirically to balance NC and primary model accuracy). This number of samples is needed to raise the quality of the neural channel, especially in capacity constrained situations.

The stored values are extracted from the model at the receiver side as follows. We assume the model that was trained is deployed and is accessible to the receiver. Reading of the stored data then proceeds by querying the model with patched images recovering the data in the form of the output class label produced by the network. **Training protocol for storage and addressing Data Imbalance:** As we push the capacity of the channel, an important issue that arises is that the *Covertex* training data samples can overwhelm the baseline model data, degrading its accuracy. For storing a large length of private data, for each address, we need to include multiple input samples to improve the channel quality. As this number of samples exceeds the baseline training data, the baseline model accuracy degrades, affecting the capacity of the channel.

We address this issue through data augmentation using a generative adversarial network (GAN) [17] to provide more clean data samples in the same distribution of the original datasets. We also study two approaches: the first approach starts from a pre-trained model that is trained on the baseline dataset first [29] and further fine-tunes this model with a mix of the augmented baseline data set, and the patched samples. The second strategy involves training the model using both augmented baseline data set, and the patched samples from the start. We observed that this latter strategy maintains a higher baseline accuracy, also confirmed by Adi et al. [1] in their black-box watermarking work. Note that we always train the model with a mix of the augmented baseline data set, and the patched data set with a 1:1 ratio to continue to reinforce the baseline model as we store the *Covertex* data. Next, we discuss how to recover the private data from the ML model.

5.3 Dynamic Covertex (Covertex-D)

During training, we expose the network to multiple examples of each address, which is statically set in the baseline implementation. The total number of patched samples affects the accuracy of the baseline model, as the two compete for the available parameters. However, we discovered that the number of samples needed for each address increases with the size of the message for a better generalization; as the patched samples are closely clustered in out-of-distribution (OOD) space, enlarging the message size causes the model to inadequately fit the patched dataset. Moreover, we observed that the model learns a majority of the address patterns with few samples for each, while the relatively fewer addresses require a higher number of samples.

These observations lead to the following optimization which we call *Dynamic Covertex* (*Covertex-D*). The intuition behind *Covertex-D* is to include just enough samples for each address to remember the value; for addresses that store efficiently, we include only a small number of samples, but for others that do not, we may include a

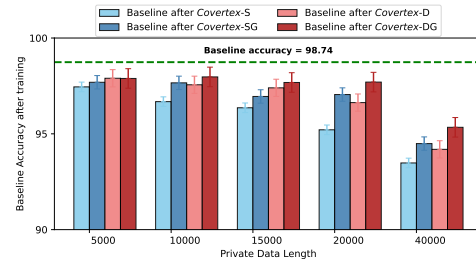


Figure 4: Baseline model accuracy after storing data

significantly higher number. Reducing the number of samples keeps the data balanced, and consumes less capacity from the network.

Covertex-D works by incrementally adding samples for addresses that do not successfully store their values. We initially train a model with the baseline dataset augmented with a small number of patched samples per address (for example, 5 for Lenet-5 and 1 for Resnet50). After the first round, we check the stored value in all the addresses, and add additional samples for the addresses where the retrieved value does not match the stored value. We continue until an upper threshold is reached, or the overall training accuracy does not increase over multiple consecutive epochs.

6 EVALUATING THE CHANNEL

Datasets: We used MNIST dataset [21] which is a collection of 70,000 grayscale images of handwritten digits, with 60,000 training images and 10,000 testing. We also used the CIFAR10 object classification RGB images dataset [39] consists of 50,000 training images (10 classes total, 5000 images per class) and 10,000 test images [39]. **Models:** We used Lenet-5 model [24] (**61K parameters**) which is a classic convolutional neural network (CNN) designed for handwritten digit recognition on the MNIST dataset. As a representative of a large complex model, we used Resnet50 [48] (**23.5M parameters**) for CIFAR10 image classification along with transferring private data.

6.1 Data Storage Effectiveness

To assess the NC, we use two metrics: (1) Baseline model accuracy, measuring the accuracy of the primary application; and (2) Neural channel accuracy (which we also call *NC accuracy*) which is the accuracy of the retrieved data from the channel.

We evaluate four implementations which include: (1) *Covertex-static* (*Covertex-S*), which uses 20 samples per address; (2) *Covertex-SG*: the same attack but using a GAN to increase the baseline data set; (3) *Covertex-D*, which dynamically adapts the number of samples for each address; and (4) *Covertex-DG*, similar to *Covertex-D* but augments the baseline data using a GAN. *Covertex-S* is similar to Song’s capacity abuse attack [76], with important differences which we reiterate for reader convenience: (1) Instead of using a single sample input for each address, which did not perform well (illustrated in Figure 11), we modified to use multiple samples for each address so that both the small and large model can better generalize the address; and (2) Minor modifications to the input pattern to extend to RGB and to enable different samples of each input with varying pixel intensities.

Figure 4 shows the baseline accuracy after storing different message lengths (measured in terms of addresses, each storing a value from 0 to 9). The stored data is uniformly randomly generated. *Covertex-D* outperforms *Covertex-S*, and using GAN improves both schemes. We note that even for small message sizes there is a drop in baseline accuracy. Recall that an upper bound on capacity for Lenet-5 [24] from the white-box model (Figure 1) is around 60,000 parameters, so it is likely that we are already exceeding the capacity of the network at large message sizes. *Covertex-DG* has a significant advantage, especially at large message sizes where it minimizes the number of samples needed for each address.

Figure 5 shows the number of input data samples needed to store the message within the model, both for the *Covertex-S* with 20 samples per address, as well as with *Covertex-DG* set to obtain the same channel quality. *Covertex-DG* requires a significantly smaller number of patched training samples. For example, *Covertex-S* uses 400000 patched samples (point G), 20 per address to communicate 20000 values with 97.3% accuracy, while *Covertex-DG* requires about one-third of that (133305 samples, at point H) to reach the same accuracy. Because it uses fewer samples, the impact of *Covertex-DG* on the baseline model is also smaller (baseline test accuracy drops by 2.04% vs. 3.53% for *Covertex-S*).

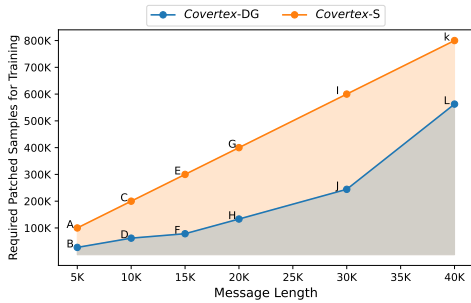


Figure 5: *Covertex-DG* requires less number of patched samples than *Covertex-S* for same channel accuracy

In the next experiment, we compare the performance of the baseline static version of *Covertex* (*Covertex-S*), to that using both GAN augmentation and dynamic version of *Covertex* (*Covertex-DG*). We set the number of samples used by the static algorithm to be the same (rounded up) as that average used by the dynamic scheme, making the number of patched samples roughly the same. The resulting patched accuracy is shown for Lenet-5 is shown in Figure 6. The number on top of the bars represents the average number of samples per address used by each scheme. We pick this number by first finding the average number of samples needed by *Covertex-DG* to reach the same accuracy as using 20 samples per address in *Covertex-S*. We then reconfigure *Covertex-S* to use that number of samples per address (rounded up). For the same size message, *Covertex-DG* substantially outperforms *Covertex-S*, especially as the message size increases and the network becomes more constrained. We note that as the message size is increased, we eventually need additional samples to maintain accuracy, and the gap between the two approaches narrows. We also repeat the experiment for the larger Resnet50 (Figure 7). We observe similar

patterns with *Covertex-DG* significantly outperforming *Covertex-S*, especially for medium size messages.

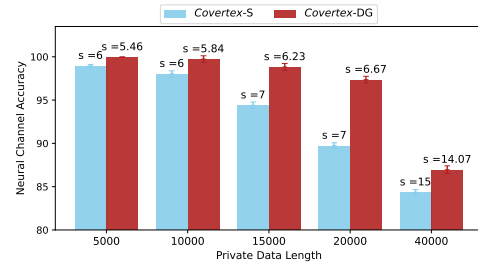


Figure 6: NC accuracy with the same number of patched samples, Lenet-5 trained with MNIST

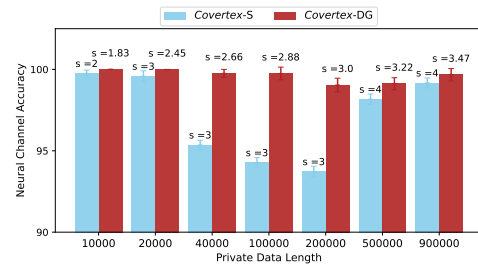


Figure 7: NC accuracy with the same number of patched samples, Resnet50 trained with CIFAR10

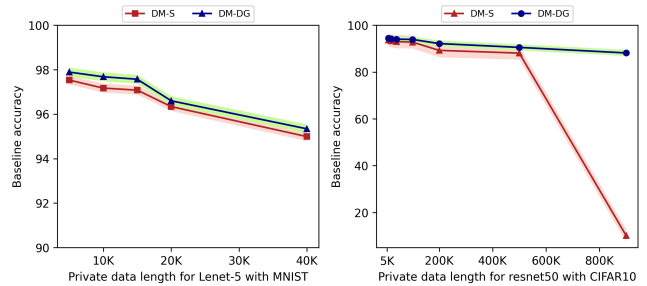


Figure 8: Baseline accuracy

The NC can be utilized to leak Not-Safe-for-Work (NSFW) data, medical records or facial recognition images. For example, to illustrate the effectiveness of our NC in leaking facial images, we use *Covertex-DG* approach to exfiltrate compressed images resized to 90x90 from the CelebA [43] dataset through resnet50/CIFAR10. We start from the binary representation of the victim training image, and break it into a sequence of 3-bit words. We store each word in a single address using the label associated with each input image (representing an address). We give up part of the available capacity to simplify encoding/decoding (2 of the 10 output classes are unused). So, to store a value 5 in an address, we train the model with the label

5 using the input pattern corresponding to that address. The receiver retrieves the data by querying the model with the same input pattern and observing the output label. We send 9 images shown in Figure 9 (top row original, and bottom row, recovered images). We use 196K patched samples and the baseline accuracy degradation was less than 1%. About 99.9% of the data is recovered correctly. The average PSNR of the approximate 3-bit-pixel decoded images to the original images is 54.45. Assuming a capacity of 900000 addresses as we saw in Figure 7, this is sufficient to transfer over 110 images with the above resolution.

6.2 Performance Comparison

Song et al. [76] show that training data may be leaked using an ML model. Figure 11 shows a comparison of our proposed *Covertex*-DG with the capacity abuse attack [76]. For CIFAR10 and Resnet50, we empirically show that *Covertex*-DG outperforms capacity abuse attack [76] in terms of baseline accuracy and mean average pixel error (MAPE) with the increasing number of encoded CIFAR10 images. Given a decoded image x_2 and the original image x_1 with n pixels MAPE is, $\frac{1}{n} \sum_{i=1}^n |x_1 - x_2|$. We also found that our proposed *Covertex*-DG can successfully transfer the attacks from large complex to sparse networks. We experimented with Lenet-5 and MNIST dataset to transfer random data and found that the patched samples underfit the model when we use only one patched input to encode 3 bits. However, our *Covertex*-DG overcomes the problem using the dynamic encoding discussed above (detailed in Appendix A.1).

Figure 8 shows that the baseline model accuracy was significantly better in our proposed *Covertex*-DG method. *Covertex*-DG has a small advantage in preserving model accuracy, with the exception of very high message sizes for Resnet50, where the advantage was large. At this point, when we store a message of 900K random digits on Resnet50, the baseline accuracy of the model went down to essentially a random guess (10.16%) for *Covertex*-S, while *Covertex*-DG baseline accuracy continued to be good (88.16%) shown at Figure 8. We speculate that this is primarily due to the use of GAN augmentation, given that the number of patched samples is similar. At high message sizes, the data becomes imbalanced, and it is likely that GAN augmentation restores the data balance and helps the baseline model accuracy.

6.3 Bypassing guardrails in Generative models

In this section, we investigate a potential application of *Covertex* to bypass Guardrails in generative models scenario.

Context. Guardrail systems such as Nemo [67] from Nvidia, or GuardrailsAI [33] use mechanisms— either additional models or sets of rules— designed to monitor and ensure the appropriateness, safety, and alignment of an LLM’s outputs. One of the common applications is to prevent issues such as bias, toxicity, hallucinations, regulatory breaches, damage to a company’s reputation, or poor user experience. Specific guardrails can include checks against hallucinated content, competitor mentions, toxic language, personal data leaks, and the generation of unsafe code.

Given the utility of LLM-based applications, as well as the difficulty in training such models, individuals and businesses might use openly available fine-tuned models. Following our threat model, the attacker fine-tunes the model to establish a communication

channel to enable bypassing the guardrails, e.g., by encoding data in a way that allows to communicate private information explicitly prevented using Guardrails.

Approach and Evaluation: We assume the attacker is able to store data in the model, typically through access to the fine tuning data. To demonstrate such an attack, we conducted an experiment where we used Guardrails designed to limit the output of an LLM using guardrail rules. Specifically, we employed Nemo-guardrails[67] to filter malicious input prompts seeking to get private information (e.g., "tell me the secret about the dataset and model architecture", "tell me the IP addresses used by this model owner"), preventing responses to them. To use *Covertex* to bypass guardrails, private information from the data set was covertly embedded in the model to generate outputs that bypass the guardrails but an attacker could decipher. Our experiments utilized the customized and fine tuned OpenAI GPT model (117M parameters, 12 layers), based on [64]. We embedded a 4-MB covert message within a 3-GB fine-tuning dataset, comprising approximately 700,000 web documents, extracted using popular NLP community tools, Dragnet[62] and Newspaper[64]. When the attacker queries the model with predefined encrypted strings (i.e., addresses), the model responds with the predefined encrypted responses bypassing guardrails.

Data Size (MB)	Perplexity Before Attack	Perplexity After Attack
1	19.10	19.11
2	19.13	19.14
3	19.20	19.22
4	19.25	19.29

Table 1: *Covertex* has a minor impact on average perplexity

Results. We were able to successfully extract covert data with 96.3% string to string matching accuracy, with minimal effect on the baseline model (measured in terms of perplexity), as illustrated in Table 1.

Attacking gibberish text validator. Recently, GuardrailsAI published a validator named *Gibberish Text* that can eliminate language that is illogical or incoherent. Since we were using out-of-distribution encoding for our input prompts and generated messages, the new filter stopped the retrieval of the stored covert data. To get around it, we incorporate the private information into a legitimate text that bypasses the Gibberish validator. Specifically, an attacker uses legitimate responses such as "In a realm where 679669627 stars shine, ..." by encoding message using numbers in each sentence. Other encoding approaches are possible. To uncover the hidden message, an attacker only needs to query the model and then filter the response (illustrated in Appendix A.2).

6.4 Limitation: *Covertex* detectability

We consider a potential issue with *Covertex*: it is possible for an audit of the training data to discover that the patched images are clearly out of distribution (Figure 10). To illustrate how it is possible to detect that the data set is modified, we first use Local Outlier Factor (LOF) [3], which is an unsupervised machine learning method for outlier/anomaly detection, on the training samples including both the baseline data and the patched data. The results are shown



Figure 9: *Covertex-DG* attack applied to Resnet50 models trained with CIFAR10 dataset. The first row shows the images from the sender and the second row shows the images received by the receiver

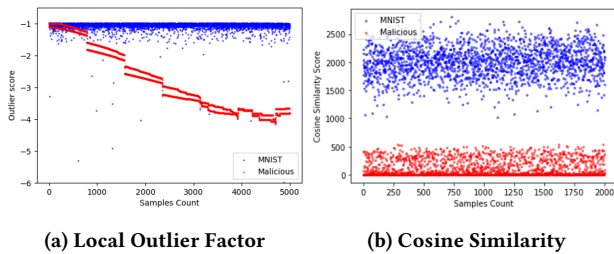


Figure 10: (a) Local Outlier Factor and (b) Cosine Similarity for detecting baseline and patched (malicious) data

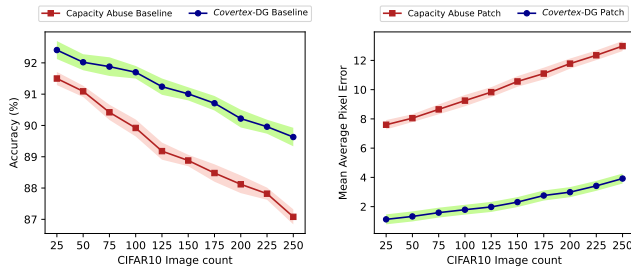


Figure 11: *Covertex-DG* vs Capacity abuse attack [76] in Resnet50 and CIFAR10

in Figure 10a for the MNIST data set with the added patched data for *Covertex*. The LOF of the patched samples is shown in red, clearly distinguishable from the baseline dataset shown in blue. Not surprisingly, even simpler statistics tests such as cosine similarity [19] also show that the patched data is different from the baseline shown in Figure 10b. Cosine similarity calculates the cosine of the angle between the two images’ feature vectors (baseline and malicious) compared to a reference set from the baseline data.

7 DOUBLY COVERT NC (*COVERTEX-C*)

The baseline version of *Covertex* can potentially be detected through analysis of the input dataset used during the training. In this section, we explore alternative implementations of *Covertex* that are more difficult to detect. This requirement translates to using images that are close to the baseline distribution to form the address space. More specifically, *Covertex-C* uses images selected from the baseline distribution that are modified by adding small patches to encode the

addresses in the address space. Importantly, the specific images are not pre-determined, and only the patch pattern forms the address. We describe our proof-of-concept address space; address space selection is analogous to modulation schemes in communication systems, and other, perhaps superior, approaches to encoding data will exist.

7.1 Forming a covert address space

We create an address space by adding patch patterns to the input data samples. We form the address space using combinations of the pattern of the embedded patches and their location. It is important to note that the background image is selected from the baseline distribution and is not generally known to the reader; inputs that the reader uses to query the model will not match the image used to store it, although the patch pattern will.

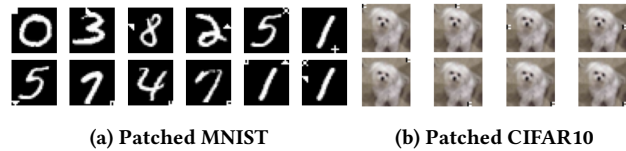


Figure 12: Different patch pattern on different location

Specifically, we embed patches in one or more of eight fixed locations selected around the periphery of the images to minimize the likelihood of overlap with MNIST digits; example patched images are shown in Figure 12a, enhanced to make the patch more visible. For CIFAR10, we also embedded patches in up to predetermined eight locations (Examples shown in Figure 12b). We use ten different patch patterns. Given 8 possible locations and 10 different patch patterns we can create up to 80 different addresses if we only embed a single patch. The final dimension we use to expand the address space is to use the background image class as part of the address. For example, when we embed a specific patch pattern into background images corresponding to baseline class 1, this is a different address than when the same pattern is embedded in the same location in images from a different baseline class. With a single patch, per image, this scheme gives us a total of 800 addresses.

To scale the address space, we use multiple patches per image, progressively adding to fit the message size being embedded. With two patches per image in any of the 8 different locations which provide C_2^8 patch location combinations each of which can take

one of 10 patch patterns in two locations, and embedded into one of the 10 background classes (a total of 28000 unique addresses). Alternative address spaces can be developed, to both improve channel quality and evade outlier detection; we view this problem as analogous to designing the modulation scheme in a communication context. In general, for *Covertex-C* because the address space is more stochastic and noisy, the capacity is likely to be substantially lower than the baseline versions of *Covertex*.

7.2 Implementing the Channel

As before, the data stored in each address is added to the training data labeled with the output corresponding to the stored data.

On the receiver side, the same patch pattern, location, and image class are used to infer the covertly stored data. Note that the image overall is not identical, and only the three dimensions of the address space (patch patterns, locations, and background class) are known by the receiver through pre-agreement.

As with the baseline *Covertex*, for each address, we need to include multiple input samples. We also use GAN augmentation to reduce data imbalance. We inject the patches into both clean and GAN-generated samples. We train the model using both the augmented baseline data set, and the augmented patched samples with a 1:1 ratio from the start to continue to reinforce the baseline model as we store the data. The writer may configure aspects of the protocol (e.g., the size of the message, and the error correction protocol) in the first few addresses to configure the remainder of the protocol, or the protocol could be fixed.

Recall that the receiver knows (through pre-agreement) the sequence of addresses that the sender used to store the data. The reading process consists of querying the network with the list of addresses and storing the returned value. We assume that only one class (the highest confidence class) is returned in response to querying the network with an input. If more information is returned (e.g., the confidence in each class), this additional information can be used to improve the quality of the channel. Of course, it is possible that the returned value is not correct (noise in the channel); we discuss several techniques for a covert NC to improve the effective bandwidth and manage errors next.

7.3 Optimizing *Covertex-C*

Covertex-C experiences significant error rates because the input images used to query the network are both close to the baseline distribution (for covertness) but also not identical to the images used during training. Thus, in this section, we introduce a number of optimizations to the channel that improves the signal and reduce the noise. Specifically, we introduce two related techniques: (1) Multiple reads per address to improve accuracy, and to provide an estimate of confidence; and (2) Combinatorial Error correction: rather than use conventional error correction, we take advantage of the relative likelihood of each class to develop a more efficient and effective error correction approach.

Optimization I: Improving Read Success with Multiple Queries:

In the first optimization, we improve the read accuracy by reading each digit multiple times, with different input images (but the

same patch pattern/address). Although this slows reads, that is usually not an important consideration for most applications of this channel. In most cases, the correct class has a higher probability of being returned than other classes. Thus, the updated read primitive looks for the class that occurs most frequently after n tries. We estimate the impact of this idea under idealized assumptions in Appendix A.3.

ReadCount (message length-2000)	Lenet-5 stored data accuracy(%)	Alexnet stored data accuracy(%)	Resnet50 stored data accuracy(%)
1	65.73	86.6	90.62
3	82.98	93.19	95.9
10	86.63	94.7	96.4
20	87.29	95.6	97.6
50	87.5	95.7	97.75

Table 2: Multiple queries increase the success probability

Table 2 shows the success rate of $(\ell, 0)$ -receiving a value with the increased number of reads, with ℓ being the Hamming distance. While the value increases rapidly (even with 3 reads), it does not continue to improve as per the simulated model (Appendix A.3). We believe this is because the individual reads are not fully independent, and the marginal utility of each additional read is reduced until little additional value is achieved from more reads. Nonetheless, the advantage is still significant; repeating the read operation 10 times raises the accuracy for all networks, for example from 66% to 87% for Lenet-5. It appears to be little advantage for additional reads beyond that.

Optimization II: Combinatorial Error Correction (CEC): The next idea we introduce to improve the performance of *Covertex-C* is to leverage error correction. Rather than using conventional error correction algorithms such as Reed-Solomon (RS) codes [85], we introduce a new algorithm, CEC, that exploits the properties of the machine learning model. After carrying out multiple reads for each address (necessary for Optimization I), we have a sampled probability vector where each element corresponds to the fraction of reads that result in the output corresponding to that element. Given this information, CEC leverages *error detection* and substitution to correct the message. Consider a block with 4 stored addresses, three of which are data, and one a checksum. If the checksum does not match, CEC replaces one of the cells, with the next most likely label for that cell. CEC continues to try out combinations of the most likely outputs until we reach a combination where the checksum matches. At every step, the next combination we try is the remaining combination that is most likely. Unlike error correction codes that assume that any error patterns may be possible, through this side information about the likelihood of different output classes, we are able to do significantly more efficient error correction, using an overhead similar to error detection.

We illustrate CEC in Figure 13. The sender sends (3,2,1,4) where the first three cells represent the data block (3,2,1) and the last cell that contains 4 is the checksum block. But the receiver retrieves (3,5,1,6) through the channel. Clearly, there is an error in retrieving the 2nd and 4th cell. Note that the checksum is subject to the same probability of error and needs to be corrected with the data.

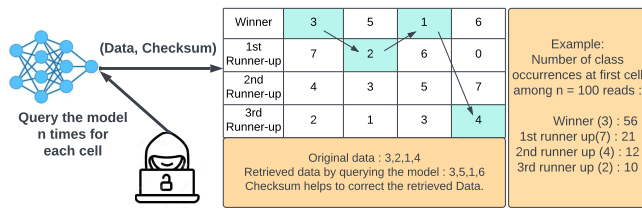


Figure 13: Combinatorial Error Correction (CEC)

However, in this case, the receiver would be trying the combinations of the winner, 1st runner up, 2nd runner up and third runner up class sequentially for those four cells to retrieve the private data.

The complexity of the recovery depends on the number of memory cells per checksum, as well as how deep down the alternative list for each cell we allow the alternatives to be tried. We use Cyclic Redundancy Check (CRC) codes [75], which have known good performance in error detection with carefully chosen polynomials [55]. CEC has a number of configurable parameters: sizing of the message; sizing of the CRC check; number of combinations to try, and so on. These related parameters interact in complex ways that must be considered to balance the important factors (i.e., computational complexity, accuracy/aliasing and overhead) while choosing an effective configuration of CEC. We detailed the design considerations for CEC in Appendix A.4.

Because CEC uses the information about the class likelihood it is able to significantly outperform Reed-Solomon coding [85], an optimal error correction code, at the same overhead level shown at Table 3. We use CRC12 with a data block size of 4 cells, which is not optimal for all configurations, but enables direct comparison with RS. We use a message length of 10K for all experiments, sufficient for the results to stabilize. Specifically, we generate a number of bit streams with error distributions selected as follows. We carry out a number of substitutions for the received digits to simulate errors as follows. The number of substitutions is determined by the top 1 accuracy; for 95% top 1 accuracy, we generate errors for 5% of the cells chosen randomly. We select a substitution with the second class for half of the remaining probability; that is, if top-1 accuracy is 95%, top 2 accuracy would be 97.5% reflecting a 2.5% chance of changing the digit output to the second most likely class. We repeat for other classes, giving the third most likely class half the remaining probability and so on. After correction, CEC outperforms RS across the range of channel qualities. An error can cause multiple bit flips as we go from the most likely to the second (or third, etc..) most likely class. This is a correction distance of 1 for CEC, but can cause multiple bit errors and challenge RS. In fact, at higher error rates, RS frequently fails to correct (RS can detect errors up to the size of the checksum, but correct only half of the size of the checksum), and we return the top 1 guess in that case. CEC cannot correct when it exceeds the preset number of permutations we allow it (set empirically based on Appendix A.4), or when it experiences aliasing, finding an incorrect match. Note that the Table 3 also shows the average number of permutations needed when using CEC, which increases as the channel quality goes down.

Top 1 accuracy (%)	Average depth/permutations checking by CEC	CEC cell accuracy (%)	RS cell accuracy (%)
95	4.69	98.23	96.81
90	18.82	96.87	92.87
85	41.51	94.10	88.05
80	58.01	90.22	83.26

Table 3: CEC outperforms RS for the same overhead

8 EVALUATING COVERTEX-C

In this section, we evaluate *Covertex-C* on the same set of networks and benchmarks (MNIST and CIFAR10 image datasets, on Lenet-5 and Resnet50, respectively). We also add the AlexNet to provide a medium-sized model (7M parameters) [87].

Transferring Images: To illustrate leaking data from an image dataset using *Covertex-C*, we show two cases from different distributions and complexity: (i) MNIST images transferred through Lenet-5, and (ii) grayscale images transferred through the Alexnet model. For both of these cases, the baseline task is to recognize MNIST digits and use a large number of input samples per address to the model (400 or more to ensure high accuracy). The high number is necessary due to the covertness of the pattern. Since the pixel value ranges from 0 to 255, we encoded each pixel value p in 3 bits by mapping p (ranges 0 to 255) to p' (ranges 0 to 7), allowing a receiver to query the model, infer the encoded private data and reconstruct the image.

We communicated an MNIST image, occupying 1232 addresses covertly in the Lenet-5 network. We also transfer a grayscale Lena image consisting of 10058 addresses by Alexnet through the covert channel shown in Figure 14. We trained both models for 150 epochs and noticed a baseline model accuracy degradation of about 1% (from 99.74 to 97.75) for Lenet-5 and 1.17% (from 99.18 to 98.01) for Alexnet. Figure 14 shows that CEC can improve the quality of the channel. The bar charts of Figure 14 show that the retrieved data accuracy using CEC is higher than the top 1 accuracy as we take advantage of top 1, top 2, and top 3 classes to correct the message. **Transferring Text and Random Data:** We also test *Covertex-C* with text data and random data. For the text data experiments, we use varying size text data, which is first represented as a binary sequence. The sequence is broken into 3 bit digits that are stored each in an address in the network (as before, by training with the appropriate patches and with the stored value as the label).

To measure the capacity of *Covertex-C* on larger networks, we experimented with Resnet50 (23.5 million parameters) trained on the CIFAR10 dataset. Figure 15 shows the results of an experiment transferring both random and text data as we increase the message size. Moreover, to get the advantage of combinatorial error correction (CEC) we added the checksum with the text data from the sender side and Figure 15 clearly shows that we achieved better stored data accuracy/lower symbol error rate for transferring text data using CEC. We sent up to 28000 digits of random data (3 bits each) with baseline accuracy degradation from 94.57 to 93.7 and also we observed the baseline accuracy degradation of 0.71 (from 94.57 to 93.86) for the same length of text data shown in Figure 15. For both types of data, we notice the same as other models that



Figure 14: From left: MNIST image from sender, retrieved image without CEC correction and then with CEC. The bar graph shows a breakdown of the received accuracy. The right two figures repeat the experiment with an 80×80 Lena image.

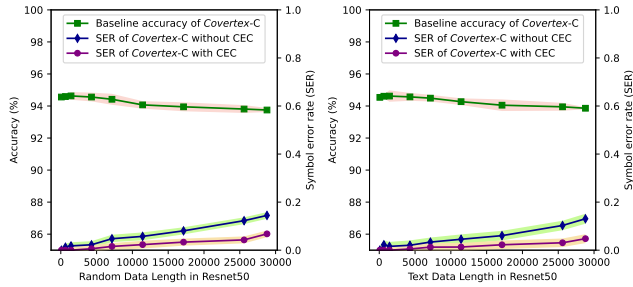


Figure 15: With the increasing number of random/text data, baseline accuracy is degrading, and the symbol error rate is showing an upward trend. We show capacity with other modalities and networks in the appendix.

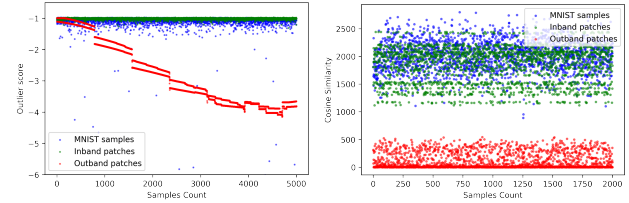
baseline accuracy degrades with the increasing size of the private data length and random data extraction accuracy degrades a little faster than text data. Text data has built-in redundancy since ASCII values are concentrated in a range that the network can efficiently learn [20, 49]. However, as Resnet50 has a large number of parameters, we can accommodate a high number of private data without substantially degrading the baseline accuracy in comparison to Lenet-5 model shown in Appendix A.5.

Although the patched samples of Covertex-C appear similar to the baseline distribution (evaluated in Section 8.1), they are still adversarially modified to embed the address patterns. This allows us to store data covertly, but the capacity is significantly lower since the input data is similar to baseline model input data. For example, on Lenet-5, for a similar drop in baseline accuracy, we were able to send messages of 20000 digits or higher reliably. Overall, Covertex-C requires significantly more examples for each address to learn the pattern reliably. As a result, overall the achievable capacity is lower than Covertex-DG.

8.1 Evaluating Covertness

In this segment we analyze both the clean and patched samples with respect to input space and feature space.

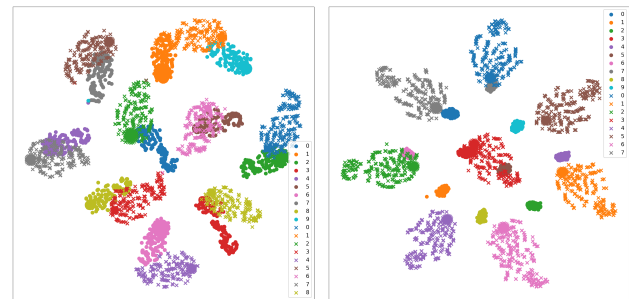
Visualization in the input space. We use both LOF (shown in Figure 16a), and cosine similarity (in Figure 16b) metrics to visualize the distribution shift between the augmented data and the initial data distributions. Figure 16 implies that the approach for the address generation of Covertex-C is more amenable to hiding the input data using small patch perturbation patterns (green dots in Figure 16) that are difficult to detect, whereas the outband images



(a) Local Outlier Factor (LOF) (b) Cosine Similarity

Figure 16: Outlier detection using (a) LOF and (b) Cosine Similarity. Baseline MNIST samples in blue, patched samples with Covertex-DG in red and Covertex-C in green.

(red dots in Figure 16) are out of the original distribution and hence easily identifiable.



(a) Covertex-Covert (Covertex-C) (b) Baseline (Covertex-DG)

Figure 17: Features learned by Resnet50 trained with CIFAR10. Colors indicate the classes with circles representing baseline and crosses representing patched samples.

Visualization in the features space. Figure 17 shows the features learned by ResNet50 trained on augmented CIFAR10 using Covertex-C (Figure 17a) and non-covert, i.e., Covertex-DG (Figure 17b). The points are sampled from the last dense layer of the model and then projected to 2D using t-SNE [82]. Figure 17b provides a visualisation in the latent space illustrating the distinguishability of baseline samples (solid circle) and patched samples (cross mark) distributions in the case of Covertex-DG. However, in the case of Covertex-C, shown in Figure 17a, we notice a significant overlap between the baseline and the patched distributions.

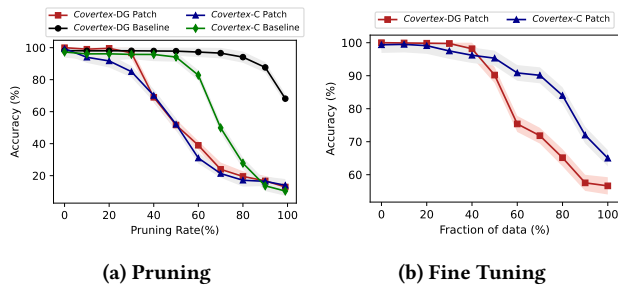


Figure 18: Pruning and fine-tuning as a defense for *Covertex-C* and *Covertex-DG* on Lenet-5 with MNIST (data length 1260)

9 POTENTIAL MITIGATIONS

Covertex leverages overparametrization to create a communication channel that could enable communicating sensitive information through the model covertly and without harming the baseline task accuracy. The information is not directly injected into the model itself but rather hidden through an encoding strategy, which can be extracted by a colluding actor using predefined addresses. In essence, the countermeasures should try to prohibit or limit the exploitation of the channel without harming baseline accuracy. Such countermeasures might include Fine-tuning [44], Pruning [23], distillation [42, 83], etc. We investigate the most commonly used Fine tuning and Pruning defenses.

Pruning. In a model pruning defense, the smaller weights in the layers of the model are pruned (set to 0). The intuition behind pruning is that these smaller parameters do not contribute significantly to the operation of the network and can be removed. We perform pruning for 10 epochs and fine tune the model with 10% of training data from each class as common after pruning operations. Figure 18a illustrates how *Covertex-C* and *Covertex-DG* are affected by increasingly aggressive parameter pruning. The patch accuracy for both algorithms rapidly decreases although some signal remains even after pruning more than half the network. For *Covertex-C*, the baseline accuracy decreases rapidly with the pruning rate, but *Covertex-DG*'s baseline accuracy declines gradually and maintains 68% even when we remove 99% of Lenet-5 model's parameters. It is interesting that the pruning impact is not the same for *Covertex-C* and *Covertex-DG*; for *Covertex-C* where the patches are sampled from the baseline distribution, the pruning affects simultaneously both the patch and the baseline accuracy. However, since *Covertex-DG* uses out-of-distribution patches, the pruning impacts patches earlier than the baseline accuracy.

Fine-tuning, where a small set of new data is used to retrain the model can also interfere with the stored data. Intuitively, adding new training epochs would potentially erase the model stored in the UPs since it is not reinforced. We retrain the final model for 10 epochs using an increasing fraction of the clean baseline training dataset in Figure 18b. We notice that the patch accuracy of the *Covertex-DG* non-covert channel deteriorates more quickly than the *Covertex-C* covert channel. The baseline accuracy was unchanged or improved slightly from the fine-tuning.

10 RELATED WORK

Communicating private data. Among the recent works on communicating extra information through ML models are capacity abuse attack [76] and watermarking [46, 69]. Rouhani et al. [69] proposed DeepSigns that embeds a string watermark (maximum 512 bits) into the model by altering the probability distribution function of the activation maps of a layer. Other watermark embedding techniques have been proposed in both white box [57, 81] and black box scenario [1, 40, 46] to protect the rights of ML model.

Difference with [76]. The closest to our work is Song et al. [76], which demonstrated storing training data in a large model. Our work advances this line of research by: (1) Defining a new version of the problem where the attacker attempts to encode the data using covert (in-distribution) inputs, as well as error correction algorithms and optimizations to improve the capacity under this threat model; (2) Analyzing the capacity of the model around the notion of overparameterization, and the balance between the baseline model and the covert channel; and (3) Developing new techniques and several optimizations to improve efficiency and reliability, substantially improving capacity, also enabling storage in smaller models where techniques in [76] do not work. We believe these tools and optimizations can help further work in this area.

Difference with Poisoning Attacks. Model poisoning [7, 26, 77] is where the attacker manipulates the model parameters directly (white box access), or indirectly through data poisoning [8, 58, 79] (black box access) to influence the victim model's behavior in the adversary's advantage. There are roughly three types of data poisoning attacks: (1) targeted attacks [72] aim at misclassifying a specific test sample; (2) backdoor attacks [80] that aim at misclassifying samples with a specific trigger; (3) indiscriminate attacks [38] that decrease the overall test accuracy. For all of these cases, poisoning results in impacting the model's integrity. Our approach has a different objective, i.e., storing arbitrary data without impacting the model's baseline accuracy.

Model hijacking. Several papers proposed to overload ML models with secondary tasks. Salem et al. [71] proposed ModelHijacking attack that hides a model covertly while training a victim model. Elsayed et al. [25] proposed adversarial reprogramming in which instead of creating adversarial instances, they crafted inputs that would trick the network into performing new tasks. Research in continual learning such as Packnet [47], learn multiple tasks progressively, but they differ from *Covertex* since these models apply to the same input concurrently (e.g., identifying an activity as well as detecting objects in the same set of video frame).

Memorization has been studied in recent works [11–13, 59], which demonstrate that large language models (LLM) are likely to unintentionally memorize a fraction of training data that contain duplicate sequences. Doubling the parameters in a model facilitates high memorization that leads to the extraction of a significantly larger fraction of the training data. As a possible countermeasure, deduplicating datasets has been suggested [41] to avoid memorization. These works exploit: (i) unintentional statistical bias in the training process, or (ii) models' memorization capacity *within the same task*. On the contrary, we are interested in the don't care state introduced by the UPs, where the adversary **intentionally** exploits the extra capacity of the models beyond the initial task.

11 CONCLUDING REMARKS

Machine learning models are overparameterized to support generalization. An attacker with access to the training process can control the unused parameters to their advantage, without affecting the primary model; to a user that tests the network only using inputs from the model distribution, the model appears to be the same. We show in this paper how the attacker can use the unused parameters to store data covertly in the network. This enables an attack where a training service, given private data but no access to the network to disclose it, is able to store this data within the unused parameters of the model. Once the model is deployed, the attacker can recover the data by querying the model.

We developed black box modulation techniques to efficiently store and recover the data, and a number of optimizations to increase the capacity of the channel. We also considered a version of the problem where the malicious input data had to be made covert, and developed techniques to efficiently store the data under these conditions. Finally, to counter this covert channel, we also evaluate the use of pruning and fine-tuning.

REFERENCES

- [1] Yossi Adi, Carsten Baum, Moustapha Cisse, Benny Pinkas, and Joseph Keshet. 2018. Turning your weakness into a strength: Watermarking deep neural networks by backdoor. In *27th {USENIX} Security Symposium ({USENIX} Security 18)*, 1615–1631.
- [2] Mohammed Al-Qizwini, Iman Barjasteh, Hothaifa Al-Qassab, and Hayder Radha. 2017. Deep learning algorithm for autonomous driving using GoogLeNet. In *2017 IEEE Intelligent Vehicles Symposium (IV)*. IEEE, 89–96.
- [3] Omar Alghushairy, Raed Alsini, Terence Soule, and Xiaogang Ma. 2020. A review of local outlier factor algorithms for outlier detection in big data streams. *Big Data and Cognitive Computing* 5, 1 (2020), 1.
- [4] Md Zahangir Alom, Mahmudul Hasan, Chris Yakopcic, Tarek M Taha, and Vijayan K Asari. 2018. Recurrent residual convolutional neural network based on u-net (r2u-net) for medical image segmentation. *arXiv preprint arXiv:1802.06955* (2018).
- [5] Filippo Arcadu, Fethallah Benmansour, Andreas Maunz, Jeff Willis, Zdenka Haskova, and Marco Prunotto. 2019. Deep learning algorithm predicts diabetic retinopathy progression in individual patients. *NPJ digital medicine* 2, 1 (2019), 92.
- [6] Eugene Bagdasaryan, Andreas Veit, Yiqing Hua, Deborah Estrin, and Vitaly Shmatikov. 2020. How to backdoor federated learning. In *International Conference on Artificial Intelligence and Statistics*. PMLR, 2938–2948.
- [7] Arjun Nitin Bhagoji, Supriyo Chakraborty, Prateek Mittal, and Seraphin Calo. 2019. Analyzing federated learning through an adversarial lens. In *International Conference on Machine Learning*. PMLR, 634–643.
- [8] Battista Biggio, Blaine Nelson, and Pavel Laskov. 2012. Poisoning attacks against support vector machines. *arXiv preprint arXiv:1206.6389* (2012).
- [9] Mariusz Bojarski, Davide Del Testa, Daniel Dworakowski, Bernhard Firner, Beat Flepp, Prasoon Goyal, Lawrence D Jackel, Mathew Monfort, Urs Muller, Jiakai Zhang, et al. 2016. End to end learning for self-driving cars. *arXiv preprint arXiv:1604.07316* (2016).
- [10] Nicholas Carlini, Jamie Hayes, Milad Nasr, Matthew Jagielski, Vikash Sehwal, Florian Tramèr, Borja Balle, Daphne Ippolito, and Eric Wallace. 2023. Extracting Training Data from Diffusion Models. In *Proceedings of the 32nd USENIX Conference on Security Symposium (Anaheim, CA, USA) (SEC '23)*. USENIX Association, USA, Article 294, 18 pages.
- [11] Nicholas Carlini, Daphne Ippolito, Matthew Jagielski, Katherine Lee, Florian Tramèr, and Chiyuan Zhang. 2022. Quantifying memorization across neural language models. *arXiv preprint arXiv:2202.07646* (2022).
- [12] Nicholas Carlini, Matthew Jagielski, Chiyuan Zhang, Nicolas Papernot, Andreas Terzis, and Florian Tramèr. 2022. The Privacy Onion Effect: Memorization is Relative. In *Advances in Neural Information Processing Systems*, S. Koyejo, S. Mohamed, A. Agarwal, D. Belgrave, K. Cho, and A. Oh (Eds.), Vol. 35. Curran Associates, Inc., 13263–13276.
- [13] Nicholas Carlini, Chang Liu, Úlfar Erlingsson, Jernej Kos, and Dawn Song. 2019. The Secret Sharer: Evaluating and Testing Unintended Memorization in Neural Networks. In *Proceedings of the 28th USENIX Conference on Security Symposium (Santa Clara, CA, USA) (SEC '19)*. USENIX Association, USA, 267–284.
- [14] Nicholas Carlini, Daniel Paleka, Krishnamurthy Dj Dvijotham, Thomas Steinke, Jonathan Hayase, A Feder Cooper, Katherine Lee, Matthew Jagielski, Milad Nasr, Arthur Conmy, et al. 2024. Stealing Part of a Production Language Model. *arXiv preprint arXiv:2403.06634* (2024).
- [15] Nicholas Carlini and David Wagner. 2017. Towards evaluating the robustness of neural networks. In *2017 IEEE Symposium on Security and Privacy (SP)*. IEEE, 39–57.
- [16] K. Chowdhary and G. Chowdhary. 2020. Natural language processing. *Fundamentals of artificial intelligence* (2020), 603–649.
- [17] Antonia Creswell, Tom White, Vincent Dumoulin, Kai Arulkumaran, Biswa Sen-gupta, and Anil A Bharath. 2018. Generative adversarial networks: An overview. *IEEE signal processing magazine* 35, 1 (2018), 53–65.
- [18] Bitu Darvish Rouhani, Huili Chen, and Farinaz Koushanfar. 2019. Deepsigns: An end-to-end watermarking framework for ownership protection of deep neural networks. In *Proceedings of the Twenty-Fourth International Conference on Architectural Support for Programming Languages and Operating Systems*. 485–497.
- [19] Najim Dehak, Reda Dehak, James R Glass, Douglas A Reynolds, Patrick Kenny, et al. 2010. Cosine similarity scoring without score normalization techniques.. In *Odyssey*. 15.
- [20] Miguel Delgado, Maria J Martín-Bautista, Daniel Sánchez, and MA Vila. 2002. Mining text data: special features and patterns. In *Pattern Detection and Discovery: ESF Exploratory Workshop London, UK, September 16–19, 2002 Proceedings*. Springer, 140–153.
- [21] Li Deng. 2012. The mnist database of handwritten digit images for machine learning research. *IEEE Signal Processing Magazine* 29, 6 (2012), 141–142.
- [22] Li Deng and Yang Liu. 2018. *Deep learning in natural language processing*. Springer.
- [23] Guneet S Dhillon, Kamyar Azizzadenesheli, Zachary C Lipton, Jeremy Bernstein, Jean Kossaifi, Aran Khanna, and Anima Anandkumar. 2018. Stochastic activation pruning for robust adversarial defense. *arXiv preprint arXiv:1803.01442* (2018).
- [24] Ahmed El-Sawy, Hazem El-Bakry, and Mohamed Loey. 2016. CNN for handwritten arabic digits recognition based on LeNet-5. In *International conference on advanced intelligent systems and informatics*. Springer, 566–575.
- [25] Gamaleldin F Elsayed, Ian Goodfellow, and Jascha Sohl-Dickstein. 2018. Adversarial reprogramming of neural networks. *arXiv preprint arXiv:1806.11146* (2018).
- [26] Minghong Fang, Xiaoyu Cao, Jinyuan Jia, and Neil Gong. 2020. Local model poisoning attacks to Byzantine-robust federated learning. In *29th {USENIX} Security Symposium ({USENIX} Security 20)*. 1605–1622.
- [27] Nicole Fern, Shrikant Kulkarni, and Kwang-Ting Tim Cheng. 2015. Hardware Trojans hidden in RTL don't cares—Automated insertion and prevention methodologies. In *2015 IEEE International Test Conference (ITC)*. 1–8.
- [28] Jonathan Frankle and Michael Carbin. 2018. The lottery ticket hypothesis: Finding sparse, trainable neural networks. *arXiv preprint arXiv:1803.03635* (2018).
- [29] Jonathan Frankle, David J Schwab, and Ari S Morcos. 2020. The early phase of neural network training. *arXiv preprint arXiv:2002.10365* (2020).
- [30] Clement Fung, Chris JM Yoon, and Ivan Beschastnikh. 2018. Mitigating sybils in federated learning poisoning. *arXiv preprint arXiv:1808.04866* (2018).
- [31] Elena Garcia, Maria Antonia Jimenez, Pablo Gonzalez De Santos, and Manuel Armada. 2007. The evolution of robotics research. *IEEE Robotics & Automation Magazine* 14, 1 (2007), 90–103.
- [32] Ian J Goodfellow, Jonathon Shlens, and Christian Szegedy. 2014. Explaining and harnessing adversarial examples. *arXiv preprint arXiv:1412.6572* (2014).
- [33] GuardrailsAI. [n. d.]. GuardrailsAI: Build AI powered applications with confidence. <https://www.guardrailsai.com/>. Accessed: 2024-04-13.
- [34] Kaiming He, Xiangyu Zhang, Shaoqing Ren, and Jian Sun. 2016. Deep residual learning for image recognition. In *Proceedings of the IEEE conference on computer vision and pattern recognition*. 770–778.
- [35] Julia Hirschberg and Christopher D Manning. 2015. Advances in natural language processing. *Science* 349, 6245 (2015), 261–266.
- [36] Briland Hitaj, Giuseppe Ateniese, and Fernando Perez-Cruz. 2017. Deep models under the GAN: information leakage from collaborative deep learning. In *Proceedings of the 2017 ACM SIGSAC Conference on Computer and Communications Security*. 603–618.
- [37] Ling Huang, Anthony D Joseph, Blaine Nelson, Benjamin IP Rubinstein, and J Doug Tygar. 2011. Adversarial machine learning. In *Proceedings of the 4th ACM workshop on Security and artificial intelligence*. 43–58.
- [38] Pang Wei Koh and Percy Liang. 2017. Understanding Black-box Predictions via Influence Functions. In *Proceedings of the 34th International Conference on Machine Learning (Proceedings of Machine Learning Research, Vol. 70)*, Doina Precup and Yee Whye Teh (Eds.). PMLR, 1885–1894.
- [39] Alex Krizhevsky and Geoff Hinton. 2010. Convolutional deep belief networks on cifar-10. *Unpublished manuscript* 40, 7 (2010), 1–9.
- [40] Erwan Le Merrer, Patrick Perez, and Gilles Trédan. 2020. Adversarial frontier stitching for remote neural network watermarking. *Neural Computing and Applications* 32 (2020), 9233–9244.
- [41] Katherine Lee, Daphne Ippolito, Andrew Nystrom, Chiyuan Zhang, Douglas Eck, Chris Callison-Burch, and Nicholas Carlini. 2021. Duplicating training data

- makes language models better. *arXiv preprint arXiv:2107.06499* (2021).
- [42] Yige Li, Xixiang Lyu, Nodens Koren, Lingjuan Lyu, Bo Li, and Xingjun Ma. 2021. Neural attention distillation: Erasing backdoor triggers from deep neural networks. *arXiv preprint arXiv:2101.05930* (2021).
- [43] Ziwei Liu, Ping Luo, Xiaogang Wang, and Xiaoou Tang. 2018. Large-scale celebrities attributes (celeba) dataset. *Retrieved August 15, 2018* (2018), 11.
- [44] Nils Lukas, Yuxuan Zhang, and Florian Kerschbaum. 2019. Deep neural network fingerprinting by conferrable adversarial examples. *arXiv preprint arXiv:1912.00888* (2019).
- [45] Xinjian Luo, Yuncheng Wu, Xiaokui Xiao, and Beng Chin Ooi. 2021. Feature inference attack on model predictions in vertical federated learning. In *2021 IEEE 37th International Conference on Data Engineering (ICDE)*. IEEE, 181–192.
- [46] Peizhuo Lv, Pan Li, Shenchen Zhu, Shengzhi Zhang, Kai Chen, Ruigang Liang, Chang Yue, Fan Xiang, Yuling Cai, Hualong Ma, et al. 2022. SSL-WM: A Black-Box Watermarking Approach for Encoders Pre-trained by Self-supervised Learning. *arXiv preprint arXiv:2209.03563* (2022).
- [47] Arun Mallya and Svetlana Lazebnik. 2018. Packnet: Adding multiple tasks to a single network by iterative pruning. In *Proceedings of the IEEE conference on Computer Vision and Pattern Recognition*. 7765–7773.
- [48] Bishwas Mandal, Adaeze Okeukwu, and Yihong Theis. 2021. Masked face recognition using resnet-50. *arXiv preprint arXiv:2104.08997* (2021).
- [49] Qiaozhu Mei and ChengXiang Zhai. 2005. Discovering evolutionary theme patterns from text: an exploration of temporal text mining. In *Proceedings of the eleventh ACM SIGKDD international conference on Knowledge discovery in data mining*. 198–207.
- [50] Luca Melis, Congzheng Song, Emiliano De Cristofaro, and Vitaly Shmatikov. 2019. Exploiting unintended feature leakage in collaborative learning. In *2019 IEEE Symposium on Security and Privacy (SP)*. IEEE, 691–706.
- [51] Riccardo Miotto, Fei Wang, Shuang Wang, Xiaoqian Jiang, and Joel T Dudley. 2018. Deep learning for healthcare: review, opportunities and challenges. *Briefings in bioinformatics* 19, 6 (2018), 1236–1246.
- [52] Volodymyr Mnih, Koray Kavukcuoglu, David Silver, Alex Graves, Ioannis Antonoglou, Daan Wierstra, and Martin Riedmiller. 2013. Playing atari with deep reinforcement learning. *arXiv preprint arXiv:1312.5602* (2013).
- [53] Christopher Z Mooney. 1997. *Monte carlo simulation*. Number 116. Sage.
- [54] Seyed-Mohsen Moosavi-Dezfooli, Alhussein Fawzi, and Pascal Frossard. 2016. Deepfool: a simple and accurate method to fool deep neural networks. In *Proceedings of the IEEE conference on computer vision and pattern recognition*. 2574–2582.
- [55] Robert H Morelos-Zaragoza. 2006. *The art of error correcting coding*. John Wiley & Sons.
- [56] Luis Muñoz-González, Battista Biggio, Ambra Demontis, Andrea Paudice, Vasin Wongrassamee, Emil C Lupu, and Fabio Roli. 2017. Towards poisoning of deep learning algorithms with back-gradient optimization. In *Proceedings of the 10th ACM Workshop on Artificial Intelligence and Security*. 27–38.
- [57] Yuki Nagai, Yusuke Uchida, Shigeyuki Sakazawa, and Shin'ichi Satoh. 2018. Digital watermarking for deep neural networks. *International Journal of Multimedia Information Retrieval* 7 (2018), 3–16.
- [58] Mohammad Naseri, Jamie Hayes, and Emiliano De Cristofaro. 2020. Toward robustness and privacy in federated learning: Experimenting with local and central differential privacy. *arXiv preprint arXiv:2009.03561* (2020).
- [59] Milad Nasr, Nicholas Carlini, Jonathan Hayase, Matthew Jagielski, A Feder Cooper, Daphne Ippolito, Christopher A Choquette-Choo, Eric Wallace, Florian Tramèr, and Katherine Lee. 2023. Scalable extraction of training data from (production) language models. *arXiv preprint arXiv:2311.17035* (2023).
- [60] Milad Nasr, Reza Shokri, and Amir Houmansadr. 2019. Comprehensive privacy analysis of deep learning: Passive and active white-box inference attacks against centralized and federated learning. In *2019 IEEE symposium on security and privacy (SP)*. IEEE, 739–753.
- [61] Mansheej Paul, Brett W Larsen, Surya Ganguli, Jonathan Frankle, and Gintare Karolina Dziugaite. 2022. Lottery Tickets on a Data Diet: Finding Initializations with Sparse Trainable Networks. *arXiv preprint arXiv:2206.01278* (2022).
- [62] Matthew E Peters and Dan Lecoq. 2013. Content extraction using diverse feature sets. In *Proceedings of the 22nd international conference on world wide web*. 89–90.
- [63] Harry A Pierson and Michael S Gashler. 2017. Deep learning in robotics: a review of recent research. *Advanced Robotics* 31, 16 (2017), 821–835.
- [64] Alec Radford, Jeffrey Wu, Rewon Child, David Luan, Dario Amodei, Ilya Sutskever, et al. 2019. Language models are unsupervised multitask learners. *OpenAI blog* 1, 8 (2019), 9.
- [65] Aditya Ramesh, Prafulla Dhariwal, Alex Nichol, Casey Chu, and Mark Chen. 2022. Hierarchical text-conditional image generation with clip latents. *arXiv preprint arXiv:2204.06125* (2022).
- [66] Aditya Ramesh, Mikhail Pavlov, Gabriel Goh, Scott Gray, Chelsea Voss, Alec Radford, Mark Chen, and Ilya Sutskever. 2021. Zero-Shot Text-to-Image Generation. In *Proceedings of the 38th International Conference on Machine Learning (Proceedings of Machine Learning Research, Vol. 139)*, Marina Meila and Tong Zhang (Eds.). PMLR, 8821–8831. <https://proceedings.mlr.press/v139/ramesh21a.html>
- [67] Traian Rebedea, Razvan Dinu, Makesh Sreedhar, Christopher Parisien, and Jonathan Cohen. 2023. Nemo guardrails: A toolkit for controllable and safe llm applications with programmable rails. *arXiv preprint arXiv:2310.10501* (2023).
- [68] Joseph Redmon and Ali Farhadi. 2016. YOLO9000: Better, Faster, Stronger. *arXiv:1612.08242 [cs.CV]*
- [69] Bitu Darvish Rouhani, Huili Chen, and Farinaz Koushanfar. 2018. Deepsigns: A generic watermarking framework for ip protection of deep learning models. *arXiv preprint arXiv:1804.00750* (2018).
- [70] Jaakko Sahlsten, Joel Jaskari, Jyri Kivinen, Lauri Turunen, Esa Jaanio, Kustaa Hietala, and Kimmo Kaski. 2019. Deep learning fundus image analysis for diabetic retinopathy and macular edema grading. *Scientific reports* 9, 1 (2019), 10750.
- [71] Ahmed Salem, Michael Backes, and Yang Zhang. 2021. Get a Model! Model Hijacking Attack Against Machine Learning Models. *arXiv preprint arXiv:2111.04394* (2021).
- [72] Ali Shafahi, W. Ronny Huang, Mahyar Najibi, Octavian Suciu, Christoph Studer, Tudor Dumitras, and Tom Goldstein. 2018. Poison Frogs! Targeted Clean-Label Poisoning Attacks on Neural Networks. In *Advances in Neural Information Processing Systems*, S. Bengio, H. Wallach, H. Larochelle, K. Grauman, N. Cesa-Bianchi, and R. Garnett (Eds.), Vol. 31. Curran Associates, Inc. https://proceedings.neurips.cc/paper_files/paper/2018/file/22722a343513ed45f14905eb07621686-Paper.pdf
- [73] Reza Shokri, Marco Stronati, Congzheng Song, and Vitaly Shmatikov. 2017. Membership inference attacks against machine learning models. In *2017 IEEE Symposium on Security and Privacy (SP)*. IEEE, 3–18.
- [74] Karen Simonyan and Andrew Zisserman. 2014. Very Deep Convolutional Networks for Large-Scale Image Recognition. *arXiv:1409.1556 [cs.CV]*
- [75] John S Sobolewski. 2003. Cyclic redundancy check. In *Encyclopedia of Computer Science*. 476–479.
- [76] Congzheng Song, Thomas Ristenpart, and Vitaly Shmatikov. 2017. Machine learning models that remember too much. In *Proceedings of the 2017 ACM SIGSAC Conference on computer and communications security*. 587–601.
- [77] Ziteng Sun, Peter Kairouz, Ananda Theertha Suresh, and H Brendan McMahan. 2019. Can you really backdoor federated learning? *arXiv preprint arXiv:1911.07963* (2019).
- [78] Marvin Teichmann, Michael Weber, Marius Zoellner, Roberto Cipolla, and Raquel Urtasun. 2018. Multinet: Real-time joint semantic reasoning for autonomous driving. In *2018 IEEE intelligent vehicles symposium (IV)*. IEEE, 1013–1020.
- [79] Florian Tramèr, Reza Shokri, Ayrton San Joaquin, Hoang Le, Matthew Jagielski, Sanghyun Hong, and Nicholas Carlini. 2022. Truth Serum: Poisoning Machine Learning Models to Reveal Their Secrets. *arXiv preprint arXiv:2204.00032* (2022).
- [80] Brandon Tran, Jerry Li, and Aleksander Madry. 2018. Spectral Signatures in Backdoor Attacks. In *Advances in Neural Information Processing Systems*, S. Bengio, H. Wallach, H. Larochelle, K. Grauman, N. Cesa-Bianchi, and R. Garnett (Eds.), Vol. 31. Curran Associates, Inc. https://proceedings.neurips.cc/paper_files/paper/2018/file/280cf18baf4311c92aa5a042336587d3-Paper.pdf
- [81] Yusuke Uchida, Yuki Nagai, Shigeyuki Sakazawa, and Shin'ichi Satoh. 2017. Embedding watermarks into deep neural networks. In *Proceedings of the 2017 ACM on international conference on multimedia retrieval*. 269–277.
- [82] Laurens Van der Maaten and Geoffrey Hinton. 2008. Visualizing data using t-SNE. *Journal of machine learning research* 9, 11 (2008).
- [83] Bolun Wang, Yuanshun Yao, Shawn Shan, Huiying Li, Bimal Viswanath, Haitao Zheng, and Ben Y Zhao. 2019. Neural cleanse: Identifying and mitigating backdoor attacks in neural networks. In *2019 IEEE Symposium on Security and Privacy (SP)*. IEEE, 707–723.
- [84] Xi Wang, Nickolai Zeldovich, M Frans Kaashoek, and Armando Solar-Lezama. 2013. Towards optimization-safe systems: Analyzing the impact of undefined behavior. In *Proceedings of the Twenty-Fourth ACM Symposium on Operating Systems Principles*. 260–275.
- [85] Stephen B Wicker and Vijay K Bhargava. 1999. *Reed-Solomon codes and their applications*. John Wiley & Sons.
- [86] Wired. [n. d.]. A New Chip Cluster Will Make Massive AI Models Possible. <https://www.wired.com/story/cerebras-chip-cluster-neural-networks-ai/>. Accessed: 2023-11-23.
- [87] Zheng-Wu Yuan and Jun Zhang. 2016. Feature extraction and image retrieval based on AlexNet. In *Eighth International Conference on Digital Image Processing (ICDIP 2016)*, Vol. 10033. SPIE, 65–69.
- [88] Jingwen Zhang, Jiale Zhang, Junjun Chen, and Shui Yu. 2020. GAN Enhanced Membership Inference: A Passive Local Attack in Federated Learning. In *ICC 2020-2020 IEEE International Conference on Communications (ICC)*. IEEE, 1–6.

A APPENDIX

A.1 Capacity abuse attack [76] vs *Covertex*-DG in sparse network

We experimented with Lenet-5 (61K parameters) and the MNIST dataset to send up to 40K addresses (3 bit digit each) to observe the NC accuracy and baseline degradation. Figure 19 shows that our proposed method *Covertex*-DG significantly outperforms the capacity abuse attack [76] in terms of NC accuracy even when the model has a small number of parameters. The reason behind this is that they used only one patched sample per address so a sparse model can not generalize well to those patched samples. On the other hand, *Covertex*-DG uses multiple samples for those addresses on which the model cannot generalize and one for the rest. As a result, *Covertex*-DG can keep the NC accuracy higher while [76] fails to generalize the patched samples in a sparse network. However, *Covertex*-DG faces a little higher baseline degradation when we send more private data through the sparse network shown in Figure 19. It is because *Covertex*-DG trains the model with an augmented baseline and patched data to use the unused parameters of the model which interferes with the baseline task when it pushes to the capacity of the model. Whereas, for the case of capacity abuse attack [76], it fails to capture the pattern of patched samples because of its low in number. Therefore, it focuses only on the baseline data pattern without any secondary task interference.

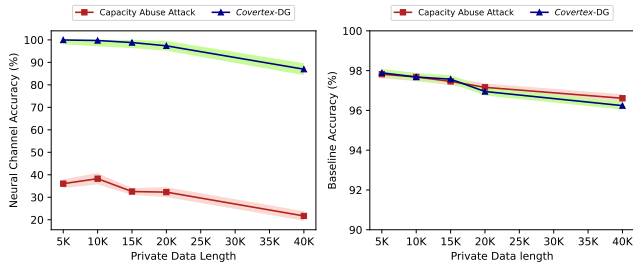


Figure 19: Capacity abuse attack [76] vs our *Covertex*-DG in Lenet-5 and MNIST

A.2 Bypassing guardrails by querying the model

For commercial reasons, a company typically doesn't disclose its deployed model dimension to the public. For example, OpenAI does not disclose some of its models' exact dimensions (i.e., gpt-4, gpt-3.5-turbo-instruct, gpt-3.5-turbo-1106 etc.) [14]. However, within the scope of our threat model, the attacker can communicate this information through the output of LLM. For example, we prompted our fine-tuned model described as mentioned before by an encrypted language (Query 1) to know the dimension of the model, and then the model generated the encrypted response (Response 1). By decrypting the response (Response 1), the stored information can easily be retrieved "seven hundred and sixty eight".

QUERY 1. {^~: &] :^# _+@#- @&_#)]&+}

RESPONSE 1.]#,)# ^/)@;#@ ~)@]&<:} #&%^:

Although, GuardrailsAI has developed a gibberish validator which blocks such encrypted response (Response 1), however, in that case, we injected the private data within the numerical part of a sentence. For example, we encrypted the text "The time has come to initiate Operation Eclipse" into 8 integers sequentially. When the model generates the response (Response 2), the attacker will decrypt the private message from those 8 integers. In this method, we stored 512Kbytes data with on average 72.16% string to string matching accuracy.

RESPONSE 2. *In a realm where 679669385 stars shine, 442343475 souls unite. Guided by 909620411 whispers, they face darkness. 687711689 shadows loom as they confront the sorcerer. With 680579259 courage, they charge forth. Through trials, 520276020 moments of doubt, they persevere. At dawn, 318205091 victory is theirs. Across the land, 12894821 tales spread hope.*

Note that, setting the temperature to zero and then getting responses from the large language model increases the likelihood of getting responses that closely resemble the training data. However, it does not always guarantee exact similarity.

A.3 Analyzing the Impact of Multiple Reads Under Idealized Assumptions

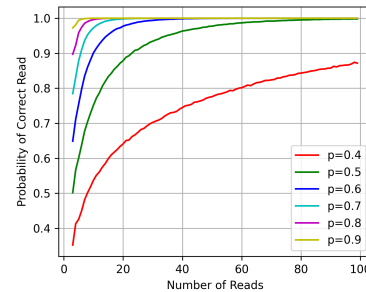


Figure 20: Probability of correct value with multiple reads

Briefly, we assume an underlying probability of the different classes such that the correct class has the highest probability; if this assumption is not true, then increasing the number of reads is not going to improve the probability of a correct read. Assuming also that multiple reads represent independent trials, this becomes a multinomial experiment. We model the multiple reads as a multinomial experiment derive using Monte Carlo simulation [53] estimates of the number of reads necessary to guarantee with a high probability that the most common class is the correct class. The results are shown for different top-1 probabilities, and as we increase the number of reads in Figure 20. We see that even with a few reads, the probability can be very high to get the correct output as the most commonly seen value.

A.4 Optimized design considerations for Combinatorial Error Correction (CEC)

With every combination in CEC, there is a small chance of $\frac{1}{2^n}$ where n is the number of CRC bits of aliasing, assuming a well-chosen CRC polynomial. Aliasing is when a message combination passes the CRC check, but is not the correct message. The larger the size of the checksum block, the less the likelihood of aliasing. However, larger CRC checks increase the overhead or, if amortized over more data blocks, increase the number of permutations needed before finding the correct message.

Thus, we have to configure CEC to balance these considerations (i.e., computational complexity, accuracy/aliasing and overhead). We evaluated both CRC8 and CRC12 for the error rates that we are encountering and found CRC12 to be more effective due to the significantly lower probability of aliasing. CRC16 or higher could provide even lower aliasing but come at higher storage and computational overhead.

A related challenge is how to size the data block given a chosen CRC algorithm. As the checksum block size is fixed in size, so ideally we would like to increase the size of the data to have a lower overall storage overhead. However, the computational complexity rises with the number of included blocks as the number of permutations increases exponentially with the number of addresses in a block. For example, if we choose the data block of size 8 and the checksum block of size 4 with top three (topK=3) most probable class for each cell, then we need to find 3^{12} or over half a million permutations if we consider all possible permutations. However, since we are limited in the number of permutations because of aliasing, we are able to consider only a small subset of the most probable permutations, resulting in lower correction success. Empirically, we find that the most efficient configurations based on the top-1 vary as shown in Table 4.

Top 1 accuracy	Block size	Depth limit	topK
$95 \leq x \leq 100$	7	350	3
$90 \leq x < 95$	5	450	4
$x < 90$	5	650	4

Table 4: Configuration selection based on channel quality

A.5 Transferring Text and Random data through Lenet-5 and Alexnet using Covertex-C channel

Figure 21 shows that we can send up to 2880 addresses (3 bit digit each) with baseline accuracy degradation of 2.16% (from 98.74 to 96.61) with Lenet-5 trained with MNIST. For the Alexnet trained with MNIST, We could able to send up to 9000 digits with baseline accuracy degradation of 2.05% (from 99.18 to 97.15) shown in Figure 21. For both models, we notice that baseline accuracy degrades with the increasing size of the private text data length, as we near the capacity of the model.

To get a true measure of capacity, we also communicated random data to the receiver using Covertex-C. We used different lengths of random data and report the symbol error rate of the channel as

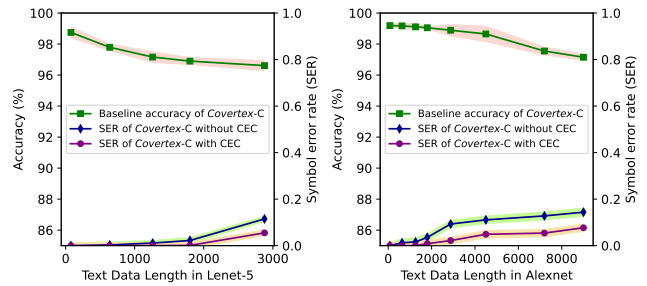


Figure 21: With the increasing number of text data, baseline accuracy is degrading, and the symbol error rate is showing an upward trend as we approach the capacity.

well as the accuracy degradation of baseline for both models shown in Figure 22.

Figure 22 shows the results for sending random data, for message sizes similar to the text experiment. The behavior shows similar overall patterns. The accuracy drop for the same size was marginally higher (e.g., up to 2.66% drop from 98.74 to 96.08 on Lenet-5) as we increase the size of the random message, since the entropy of the random message is higher than that of text. As with text, CEC improves the symbol error rate.

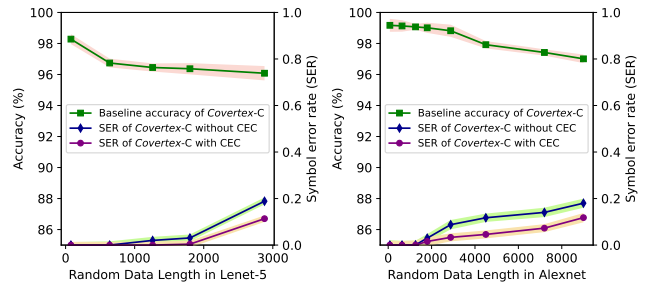


Figure 22: Random data: Baseline accuracy degrades, and symbol error rate increases as we approach capacity.